Connection between microstructural alterations detected by diffusion MRI and cognitive dysfunction in MS: A model-free analysis approach

Péter Faragó [a], Eszter Tóth [a,b], Nikoletta Szabó N [a], Krisztián Kocsis [a,b], Bálint Kincses [a,c], Bence Bozsik [a], Dániel Veréb [b], Tamás István Biernacki [a], András Király [a,b], Dániel Sandi [a], Krisztina Bencsik [a], Péter Klivényi [a], László Vécsei [a,d], Zsigmond Tamás Kincses [a,b,*]

[a] Department of Neurology, Albert Szent-Györgyi Clinical Center, University of Szeged, Szeged, Hungary
[b] Department of Radiology, Albert Szent-Györgyi Clinical Center, University of Szeged, Szeged, Hungary
[c] Department of Psychiatry, Albert Szent-Györgyi Clinical Center, University of Szeged, Szeged, Hungary
[d] MTA-SZTE Neuroscience Research Group and Intersdisciplinary Excellence Centre

ARTICLE INFO

ABSTRACT

Background: Cognitive decline is a prominent symptom of MS. Clear connection between cognitive status and white matter microstructural changes has not been unequivocally observed to date.
Objective: To characterise the relationship between white matter microstructure and cognitive performance a partial least squares (PLS) approach was used.
Methods: 53 RR MS patients' T1 and DTI images and BICAMS subtests were used in our analysis. Standard FSL pipeline was used to obtain diffusion parameters. A PLS approach was applied to reveal the diffusion parameter patterns responsible for the cognitive dysfunction.
Results: The first latent variable (LV) was mainly associated with demyelination, while the second and third explained axonal damage. While the first two LV represented mainly Brief Visuospatial Memory Test (BVMT) and Single Digit Modality Test (SDMT), the third LV depicted diffusion alterations mainly the verbal subtest. The first LVs spatial map showed demyelination in the corpus callosum. The second LVs spatial map showed the diffusion alterations in the thalamus. The third LV depicted diffusion alterations in the putative left superior longitudinal fascicle.
Conclusion: Visual memory demanding tasks versus language functions depend on distinct patterns of diffusion parameters and the spatial organisation. Axial diffusivity alterations, a putative marker of irreversible axonal loss explained around 20% of variability in the cognitive functions.

1. Introduction

Multiple sclerosis (MS) is a chronic demyelinating disease of the central nervous system. Its most frequent radiological manifestation is the appearance of the well-known T2-hyperintense white matter lesions (Montalban et al., 2018), however grey matter atrophy (Kincses et al., 2014; De Stefano et al., 2016; Toth et al., 2017) and microstructural disintegration of the normal appearing white matter (NAWM) (Roosendaal et al., 2009) are also observable.

Clinically, functional disability is prevalent and monitored using the Expanded Disability Status Scale (EDSS) (Kurtzke, 1983). Cognitive decline is also observed in MS (Strober et al., 2018), which can be revealed by neuropsychological assessment. The Brief International

Cognitive Assessment for MS (BICAMS) is a collection of cognitive tasks (Walker et al., 2016) containing three subtests: (I) the Symbol Digit Modality Test (SDMT) is a simple substitution task for measuring information processing efficiency, (II) the Brief Visuospatial Memory Test (BVMT) is used for visuospatial memory evaluation, and (III) the California Verbal Learning Test (CVLT) measures verbal learning and memory. BICAMS has been validated and is being used for evaluation of cognitive performance in several languages (Sousa et al., 2018; Sandi et al., 2015).

Previous reports revealed associations between cognitive impairment and MRI parameters. Lesion burden and localisation is a weak predictor of cognitive functions (ZT Kincses et al., 2011). Several studies showed that various measures of global and focal brain atrophy

---

Table 1
Demographic data of the participants and the cognitive tests.

	Demographic data of the patients (mean ± STD)
n (male)	53 (Behrens et al., 2003)
age (years)	41.69 ± 10.96
disease duration (years)	11.87 ± 9.85
EDSS	1.7 ± 1.65
SDMT value	43.5 ± 11.4
BVMT value	21.8 ± 7.9
CLVT value	53.5 ± 9.5

correlate with cognitive dysfunction in MS (Frau et al., 2018; Sormani et al., 2018; Damjanovic et al., 2017), but grey matter atrophy cannot explain the full scale of physical and cognitive decline on its own. The demyelination process in MS is extensive, appears in the lesions as well as in the NAWM (Toth et al., 2017; Kincses et al., 2020). Despite the concurrent cognitive decline and white matter pathology, the relationship between microstructural disintegration and cognitive function was only sparsely investigated (Tóth et al., 2019).

In our study, we aimed to find connection between BICAMS, the most frequently used cognitive test package and the pattern of DTI parameter alterations in MS. We aimed to identify patterns of the various diffusion parameters that is behind the cognitive dysfunction with a model-free approach of partial least squares (PLS). This method is also able to provide insight into the common pathology driving various cognitive functions.

2. Materials and methods

2.1. Subjects

Fifty-three relapsing-remitting multiple sclerosis patients were included in our study. All the patients were recruited from the MS Outpatient Clinic of the Department of Neurology, University of Szeged. The diagnoses were set up by MS specialists, based on the revised McDonald criteria (Polman et al., 2005). All the patients received disease-modifying therapy and were in a clinically stable condition with no relapses recorded within 6 months before and after scanning. The detailed demographic data is depicted in *Table 1*.

The local ethics committee of the Medical University of Szeged approved the study (No. 56/2011). All participants gave their written informed consent in accordance with the Declaration of Helsinki.

2.2. Cognitive testing

All subtests (SDMT, CVLT, BVMT) of the BICAMS were acquired from all the patients.

The SDMT measures information processing speed. Pseudorandomized lines contain nine different symbols, which represent different digits. The correspondence between symbols and digits is attached to the task. The patients have to pair as many symbols with the corresponding digit as they can in 90 s. There is both written and oral version of the test, however, they measure the same function. Oral version was used in our study.

For the measurement of verbal learning, CVLT is a valid tool. During the test administration, the patients have to recall as many words as they can by repeating them back. The list contains 16 words in four semantic groups. The examiner reads the words during the test at approximately 1 word/second speed. There is no time limit for this test. In our study, we used CVLT alongside with the BICAMS validated data.

BVMT or BVMT-R measures the visual memory of the patients. The test administrator shows the participant a matrix of six abstract figures for ten seconds. The participant has to reproduce them on a blank paper as accurately as they can. There is no time limit for the test.

Cognitive tests were carried out by one of the MS experts, a trained medical nurse or resident. The BICAMS test result scores were used in the further analysis steps.

2.3. Image acquisition

MR imaging was carried out on a 1.5 T GE Signa Excite HDxt scanner. High resolution T1-weighted (FSPGR: TE: 4.1 ms, TR: 10.276 ms, matrix: 256 × 256, FOV: 25 × 25 cm, Flip angle: 15°, in-plane resolution: 1 × 1 mm, slice thickness: 1 mm), FLAIR (TE: 133 ms, TR: 6000 ms, TI: 1848 ms, matrix: 256 × 256, FOV: 25 × 25 cm, Flip angle: 90°, in-plane resolution: 1 × 1 mm, slice thickness: 1 mm) and 60 direction diffusion-weighted images with 6 non-diffusion-weighted reference volumes (TE: 93.8 ms, TR: 16,000 ms, matrix: 96 × 96, FOV: 23 × 23 cm, Flip angle: 90°, in-plane resolution: 2.4 × 2.4 mm slice thickness: 2.4 mm, b: 1000s/mm2, NEX: 2, ASSET) were acquired for each patient. During the scanning noise was attenuated by earplugs and the head of the patients was restricted by foam pads.

2.4. DTI pre-processing

All pre-processing steps were performed using FSL (FMRIB software library, http://www.fmrib.ox.ac.uk/fsl). DTI data were corrected for eddy currents and movement artifacts by twelve degrees-of-freedom linear registration to the first non-diffusion weighted image for each image. Then, the non-brain part of the images was extracted by FSL's brain extraction tool. The parameters (mean diffusivity - MD, axial diffusivity - AD, radial diffusivity - RD and fractional anisotropy - FA) were estimated using the FDT tool (Behrens et al., 2003).

Tract-based spatial statistics (TBSS) was used to reduce the misalignment errors and register all the images into common space (Smith et al., 2006). All subjects' FA images were aligned to the 1 mm isovoxel FMRIB58_FA standard space template with non-linear registration using a b-spline representation of the registration warp field. The standardized FA images were skeletonized, then thresholded to 0.2 probability. The resulting FA skeleton represents the group-wise central part of the white matter tracts. All subjects' FA image was projected onto this skeleton, resulting in a 4D skeletonized image. The remaining diffusion data (radial diffusivity, axial diffusivity and mean diffusivity) was also projected onto this skeleton using the previously generated warp fields.

2.5. Partial least squares (PLS) analysis

The multivariate partial least squares (PLS) analysis was carried out by the Baycrest's lab PLS software (McIntosh and Lobaugh, 2004). PLS is a statistical method that computes the optimal least-square fit to a part of the covariance matrix. It fits a linear regression model between the variables by decomposing them into new latent variables (LVs), which are conversely independent. The analysis can also compute the cross-block covariance between the design matrix containing the conditions (scores on the cognitive tests) and the "intensity" (diffusion parameters) of the voxels in all images for all subjects.

If (n) is the number of subjects, (k) represents the number of tests, the data measured from (m) number of voxels at (t) diffusion parameters, then the cross-block covariance matrix is: $Y=C^T*M/(n*k-1)$, where M symbolizes an *(n*k by m*t)* data matrix, furthermore C is the orthogonal *(n*k by k-1)* contrast matrix. The superscript T represent the matrix transpose. This cross-block covariance matrix is put through singular value decomposition: $svd(Y^T)= U*S*V^T$, where U is a *(m*t by k-1)* matrix containing voxel saliences. V is a *(k-1 by k-1)* matrix containing design saliences. S is containing *(k-1)* nonzero singular values. The pair of the design and voxel saliences makes a latent variable, which describes the connection between the spatial pattern of diffusion parameters and the cognitive functions.

The statistical inference on the significance of the latent variables was carried out by permutation and bootstrap tests (included in the PLS software). In the first case, the labels of the design were reordered

Table 2

Localisation of maxima voxels of the latent variable's cluster in MNI152 space.

		x coordinate	y coordinate	z coordinate
LV1				
positive z values	cluster 1	77	136	66
	cluster 2	98	67	41
	cluster 3	123	47	86
	cluster 4	106	76	68
	cluster 5	83	94	50
negative z valuses	cluster 1	91	141	92
	cluster 2	118	68	90
	cluster 3	115	85	99
	cluster 4	109	170	69
	cluster 5	69	79	98
LV2				
positive z values	cluster 1	114	54	99
	cluster 2	111	98	118
	cluster 3	77	114	59
	cluster 4	101	120	65
	cluster 5	68	46	101
negative z valuses	cluster 1	80	114	86
	cluster 2	113	80	97
	cluster 3	101	101	67
	cluster 4	72	98	72
	cluster 5	85	112	71
LV3				
positive z values	cluster 1	120	63	95
	cluster 2	114	88	64
	cluster 3	120	68	110
	cluster 4	129	79	90
	cluster 5	107	116	71
negative z valuses	cluster 1	94	88	83
	cluster 2	75	100	44
	cluster 3	63	119	61
	cluster 4	58	130	80
	cluster 5	67	121	97

randomly, and the singular value decomposition was computed again for all cross-block covariance matrix (2000 times). In order to test for the stability of the results we used bootstrapping. Random sample with replacement was used and PLS was recalculated repetitively (500 bootstrapping steps). Significant clusters on the spatial maps were identified by FSL's cluster command ($Z>2.3$).

3. Results

The three subtests of the BICAMS test were used as separate covariates in our analysis. The PLS analysis found twelve LVs. After the permutation and bootstrap testing, the first three LVs were identified as significant ($p<0.05$) and showed at least 5 percentage cross-block correlation. In the following sections we will only consider these.

The voxel saliences were set to a significance level of $p<0.05$ value as determined by the bootstrapping analysis. After cluster analysis, arbitrarily, only the five clusters greatest in intensity and size were represented in each LV for voxel salience representation. The bootstrapping ratio resulted positive and negative z-scores, representing positive or negative effect to the correlations, both positive and negative thresholding was applied. The coordinates of peak intensity of each cluster was depicted to Table 2.

3.1. Latent variable #1

The first latent variable explained 63% cross-block correlation. The latent variable was represented by the following diffusion parameter correlations: FA: SDMT: $r=-0.57$; BVMT: $r=-0.49$; CVLT: $r=-0.38$; AD: SDMT: $r = 0.35$; BVMT: $r = 0.63$; CVLT: $r = 0.42$; MD: SDMT: $r = 0.49$; BVMT: $r = 0.49$; CVLT: $r = 0.42$; RD: SDMT: $r = 0.53$; BVMT: $r = 0.5$; CVLT: 0.41.

The corresponding voxel saliences represented the negative z-scores,
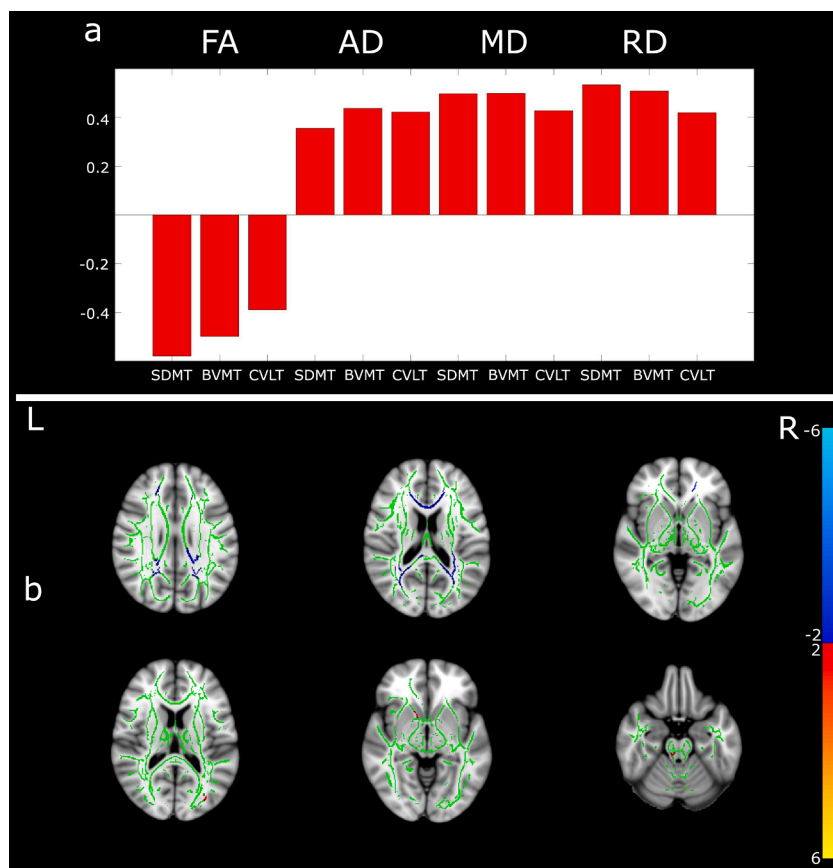

Fig. 1. The correlation values and the spatial distribution of the first latent variable. The effect of the cognitive tests and their connection to the diffusion parameters are shown in Figure1a. The Y axis and represents the correlation values (r values) between diffusion parameters (upper row X axis) and cognitive scores (lower row X axis). The voxel saliences (e.g. spatial distribution) of the significant area shown in Figure 1b. The threshold of the spatial maps was set to 2, depicted red to yellow and −2 to negative scores depicted in blue-lightblue..
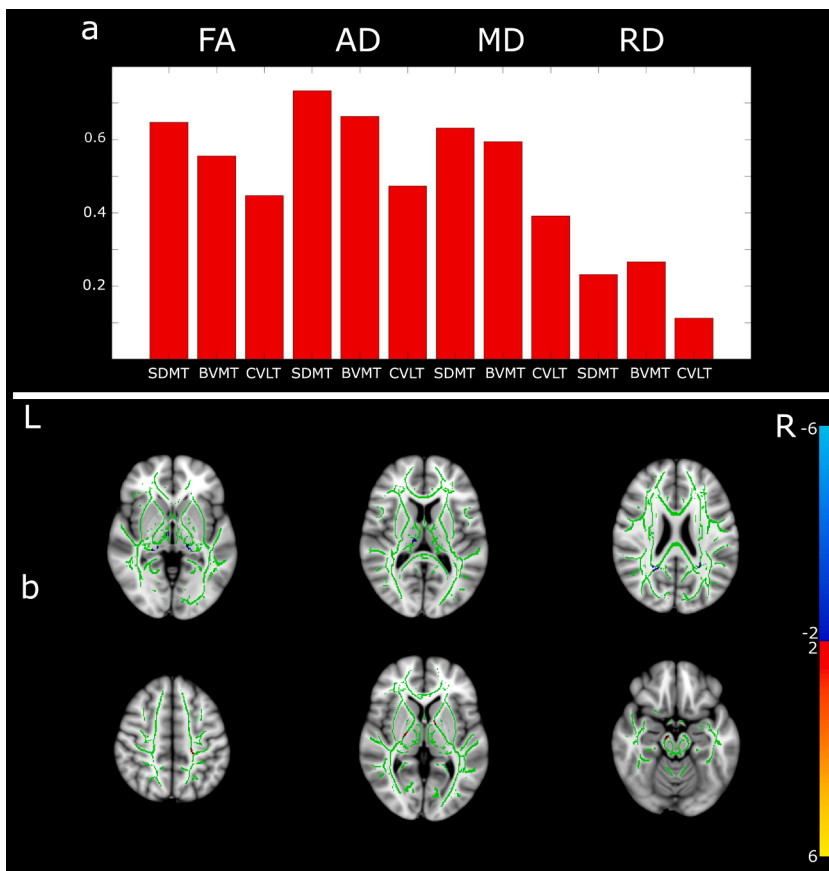
Fig. 2. The correlation values and the spatial distribution of the second latent variable. The effect of cognitive tests and their connection to the diffusion parameters are shown in Figure1a. The Y axis represents the correlation values (r values) between diffusion parameters (upper row X axis) and cognitive scores (lower row X axis). The voxel saliences (e.g. spatial distribution) of the significant area shown in Figure 2b. The lower threshold of the spatial maps was set to 2, depicted red to yellow and −2 to negative scores depicted in blue-lightblue..

wich were localised in the anterior corpus callosum, right frontal white matter next to the premotor area, left frontobasal white matter and both side in the deep parietal white matter. Positive z-scores were revealed in the right and anterior internal capsule, left occipital white matter and left cerebellar white matter.

The detailed area of correlation and r values depicted at Fig. 1.

3.2. Latent variable #2

The second latent variable explained 20,5% cross-block correlation. The latent variable revealed highest correlation coefficients between FA: SDMT: $r = 0.64$; BVMT: $r = 0.55$; CVLT: $r = 0.44$; AD: SDMT: $r = 0.73$; BVMT: $r = 0.66$; CVLT: $r = 0.47$; MD: SDMT: $r = 0.63$; BVMT: $r = 0.59$; CVLT:$r = 0.39$; RD: SDMT: $r = 0.23$; BVMT:$r = 0.26$; CVLT: 0.11.

The voxel saliences represented negative z-scores, which were localised in the posterior corpus callosum and parietal white matter, right central thalamic white matter and both sided posterior thalamic white matter. Positive z-scores were present in left frontal white matter next to the primer motor area, right mesencephalic white matter and both internal capsule. The r-values of the correlations and area of differences depicted at Fig. 2.

3.3. Latent variable #3

The third latent variable was responsible for 5,9% variance of the cross-block correlation. The latent variable revealed highest correlation coefficients was FA: SDMT: $r = 0.35$; BVMT: $r = 0.34$; CVLT: $r=-0.46$; AD: SDMT: $r=-0.28$; BVMT: $r=-0.17$; CVLT: $r = 0.59$; MD: SDMT: $r=-0.34$; BVMT: $r=-0.25$; CVLT: $r = 0.53$; RD: SDMT: $r=-0.36$; BVMT: $r=-0.29$; CVLT: 0.49.

The highest negative voxel saliences were localised in the upper brainstem on the left side, right hippocampal white matter, right internal capsule and posterior corpus callosum. Positive z-scores were found in the left motor pathway in the internal capsule, left temporal white matter, left arcuate fasciculus and in the left occipito-parietal white matter. The results showed in Fig. 3.

4. Discussion

Our model-free analysis provides evidence for connection between MRI diffusion parameters and cognitive performance in multiple sclerosis. The results pointed out that (i) diffusion parameters predicting performance on SDMT and BVMT tests could be well separated from those related to CVLT and (ii) patterns of diffusion parameters representing demyelination and axonal damage in certain spatial arrangements corresponds to cognitive dysfunctions.

White matter microstructural disintegration is a well-known phenomenon in MS (Aliotta et al., 2014; Giorgio et al., 2010). As reported in several studies, there is a well-established connection between structural MR markers and cognitive performance. Previous studies have demonstrated that the different patterns of the diffusion parameter alterations may indicate various pathological white matter changes. It was shown that, the changes in axial and radial diffusivity relate to axon or myelin damage, respectively (Velicu et al., 2012; Song et al., 2005; Nocentini et al., 2012). It was shown that fractional anisotropy and axial diffusivity correlated with the total number of axons (Montalban et al., 2009). In a combined cuprizone-induced demyelination and experimental autoimmune encephalomyelitis axonal damage and cellular infiltration was related to the alteration of axial diffusivity, whereas demyelination after cuprizone treatment caused changes in radial diffusivity, but not in axial diffusivity (Perez-Miralles et al., 2009). Postmortem human investigations showed that myelin content was predicted by the changes in radial diffusivity, fractional anisotropy and mean diffusivity (Senda et al., 2012). Accordingly, the first LV in our investigation represented
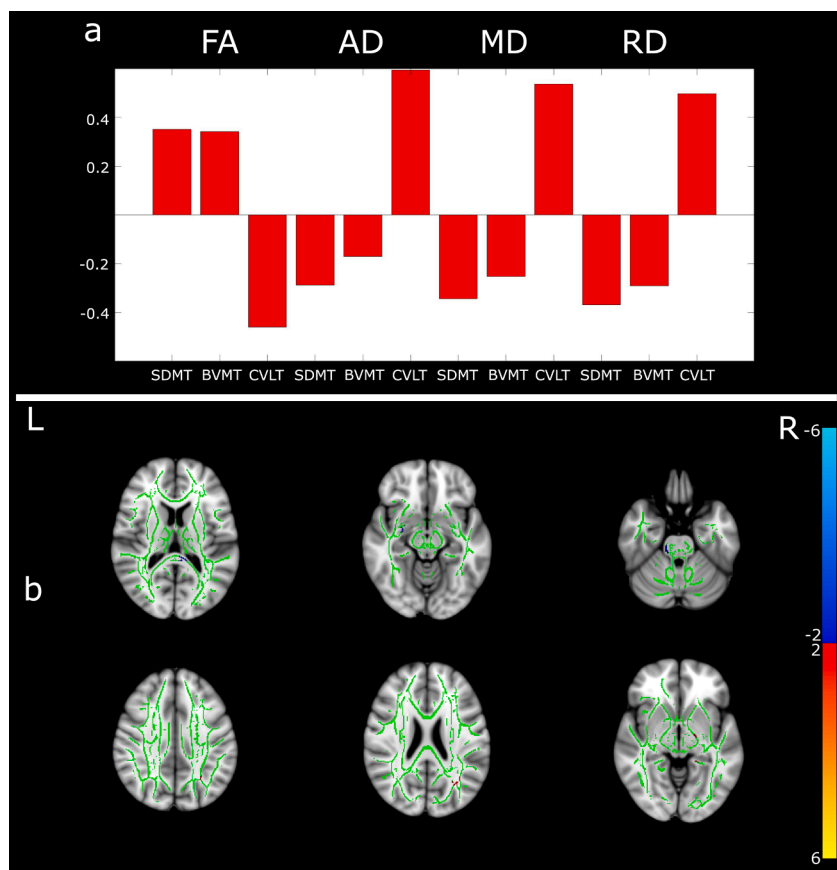
Fig. 3. The correlation values and he spatial distribution of the third latent variable. The effect of cognitive tests and their connection to the diffusion parameters are shown in Figure1a. The Y axis and represents the correlation values (r values) between diffusion parameters (upper row X axis) and cognitive scores (lower row X axis). The voxel saliences (e.g. spatial distribution) of the significant area shown in Figure 3b. The lower threshold of the spatial maps was set to 2, depicted red to red and −2 to negative scores depicted in blue-lightblue.

changes in all diffusion parameters (FA, MD, AD and RD), but slightly lower for AD. If AD and RD changed with the same magnitude, FA would have not been altered. Hence, spatial pattern reflected by the constellation of diffusion parameters is more likely driven by demyelination represented by higher correlation values for RD. Contrary, LV2 depicted changes in FA, AD and MD, a putative signature of axonal loss. LV3 showed slightly similar pattern as LV2, higher correlation values for AD most probably depict predominantly axon loss.

Importantly, LV2 accounted for approximately 20% of variability of the cross-block correlation matrix, meaning one quarter of the cognitive impairment's variance may be explained by putative axonal damage, which has presumably little potential for regeneration.

Another aspect of our findings is the pattern of cognitive dysfunctions. LV1 and LV2 represented diffusion parameter pattern for all three cognitive functions but least importantly for CVLT. On the contrary LV3 depicted the microstructural alterations for the language function.

The relationship of white matter diffusion parameters and cognitive dysfunction have been investigated, however, reports are controversial. Some studies found connection to clinical disability (Filippi et al., 2001; Onu et al., 2012; Ciccarelli et al., 2001), whereas others did not (Griffin et al., 2001; Hasan et al., 2005). It is important to note that these studies used the EDSS, a widely used clinical scale measuring multiple domains as a descriptive measure of clinical condition. EDSS includes a summarized assessment of cognitive function, but it does not measure different aspects of it in detail, even though cognitive impairment is similarly, if not more important than physical disability in the progression of MS (Fricska-Nagy et al., 2016). Impaired cognitive performance in various domains such as verbal fluency (Blecher et al., 2019), information processing speed (Abel et al., 2019; Johnen et al., 2019) or multiple cognitive tests (Baumeister et al., 2019) was also associated with white matter pathology, although these studies mostly used ROI based approaches.

In our multivariate analysis, correlation with MS patients' diffusion parameters showed distinct patterns in the case of BVMT and SDMT, and CVLT. The diffusion changes associated with CVLT amongst others showed a pattern involving the left parietal white matter corresponding to the putative superior longitudinal fascicle. This pattern is similar to what we have found in our earlier study describing correlation between language functions (verbal fluency) and lesions appearing in the left parietal white matter (ZT Kincses et al., 2011). If we incorporated other structural measures CVLT was also related to the volume of the right hippocampus (Toth et al., 2019).

A distributed pattern of diffusion alterations in case of SDMT and BVMT for LV1 and LV2 might be related to the distributed network of brain regions behind these complex cognitive tasks. The corpus callosum, the major white matter interconnecting structure emphasize the importance of these distributed networks. Similarly the thalamus is the major subcortical structure orchestrating brain functions in distributed cortical regions.

It is important to point out that the current analysis concentrated only on the diffusion parameters of the white matter. In a previous publication of our lab, using a similar PLS analysis, we investigated the connection between various structural MRI markers behind the BICAMS subtests (Tóth et al., 2019). It has to be pointed out that white matter diffusion parameters explain only part of the cognitive dysfunction in MS and the individual MRI markers might not even be independent (Toth et al., 2017).

The primary usage of PLS is the analysis of signal from functional imaging and evoked potential data (McIntosh et al., 1996; Ge et al., 2017; Vytvarova et al., 2017). A modified implementation of PLS is also suitable for analysis of structural MRI alterations connected to behavioural data, such as cognitive test results (Konukoglu et al., 2016; Park et al., 2015). More importantly, the approach has its major advantage in structural data such as DTI, in which multiple, not entirely independent

parameters are describing tissue microstructure. Hence the pattern of diffusion parameters defining the cognitive dysfunction over multiple tests can be depicted and related to spatial distributions.

5. Conclusion

Microstructural damage of the white matter, not detectable on conventional imaging plays a crucial role in the cognitive dysfunction appearing in MS. The DTI approach has the advantage to differentiate between two major pathological processes in the white matter. With further research into the field, the in depth evaluation of contribution of the axon loss and demyelination may be used to help to stratify the therapy of MS patients.

CRediT authorship contribution statement

Péter Faragó: Conceptualization, Formal analysis, Methodology, Writing – original draft, Funding acquisition. **Eszter Tóth:** Data curation, Project administration, Writing – review & editing. **Nikoletta Szabó N:** Conceptualization, Data curation, Formal analysis. **Krisztián Kocsis:** Data curation, Methodology. **Bálint Kincses:** Data curation, Investigation, Conceptualization. **Bence Bozsik:** Conceptualization, Data curation. **Dániel Veréb:** Conceptualization, Data curation, Formal analysis, Writing – original draft, Visualization. **Tamás István Biernacki:** Conceptualization, Data curation, Writing – review & editing. **András Király:** Conceptualization, Data curation, Formal analysis. **Dániel Sandi:** . **Krisztina Bencsik:** Conceptualization, Data curation, Validation. **Péter Klivényi:** Conceptualization, Funding acquisition, Supervision. **László Vécsei:** Conceptualization, Data curation, Writing – review & editing. **Zsigmond Tamás Kincses:** Conceptualization, Writing – review & editing, Supervision, Funding acquisition.

Declaration of Competing Interests

The author(s) declared no potential conflict of interest with respect to the research, authorship and/or publication to this article.

References

Montalban, X., Gold, R., Thompson, A.J., Otero-Romero, S., Amato, M.P., Chandraratna, D., 2018. ECTRIMS/EAN guideline on the pharmacological treatment of people with multiple sclerosis. Eur. J. Neurol. 25 (2), 215–237.

Kincses, Z.T., Toth, E., Banko, N., Vereb, D., Szabo, N., Csete, G., 2014. Grey matter atrophy in patients suffering from multiple sclerosis. Ideggyogy Sz 67 (9–10), 293–300.

De Stefano, N., Stromillo, M.L., Giorgio, A., Bartolozzi, M.L., Battaglini, M., Baldini, M., 2016. Establishing pathological cut-offs of brain atrophy rates in multiple sclerosis. J Neurol Neurosur Ps 87 (1), 93–99.

Toth, E., Szabo, N., Csete, G., Kiraly, A., Farago, P., Spisak, T., 2017. Gray Matter Atrophy Is Primarily Related to Demyelination of Lesions in Multiple Sclerosis: a Diffusion Tensor Imaging MRI Study. Front Neuroanat 11, 23.

Roosendaal, S.D., Geurts, J.J., Vrenken, H., Hulst, H.E., Cover, K.S., Castelijns, J.A., 2009. Regional DTI differences in multiple sclerosis patients. Neuroimage 44 (4), 1397–1403.

Kurtzke, J.F., 1983. Rating neurologic impairment in multiple sclerosis: an expanded disability status scale (EDSS). Neurology 33 (11), 1444–1452.

Strober, L., DeLuca, J., Benedict, R.H., Jacobs, A., Cohen, J.A., Chiaravalloti, N., 2018. Symbol Digit Modalities Test: a valid clinical trial endpoint for measuring cognition in multiple sclerosis. Mult. Scler. 1352458518808204.

Walker, L.A., Osman, L., Berard, J.A., Rees, L.M., Freedman, M.S., MacLean, H., 2016. Brief International Cognitive Assessment for Multiple Sclerosis (BICAMS): canadian contribution to the international validation project. J. Neurol. Sci. 362, 147–152.

Sousa, C., Rigueiro-Neves, M., Miranda, T., Alegria, P., Vale, J., Passos, A.M., 2018. Validation of the brief international cognitive assessment for multiple sclerosis (BICAMS) in the Portuguese population with multiple sclerosis. BMC Neurol. 18 (1), 172.

Sandi, D., Rudisch, T., Fuvesi, J., Fricska-Nagy, Z., Huszka, H., Biernacki, T., 2015. The Hungarian validation of the Brief International Cognitive Assessment for Multiple Sclerosis (BICAMS) battery and the correlation of cognitive impairment with fatigue and quality of life. Mult Scler Relat Disord 4 (6), 499–504.

Kincses, Z.T., Ropele, S., Jenkinson, M., Khalil, M., Petrovic, K., Loitfelder, M., 2011a. Lesion probability mapping to explain clinical deficits and cognitive performance in multiple sclerosis. Mult. Scler. 17 (6), 681–689.

Frau, J., Fenu, G., Signori, A., Coghe, G., Lorefice, L., Barracciu, M.A., 2018. A cross-sectional and longitudinal study evaluating brain volumes, RNFL, and cognitive functions in MS patients and healthy controls. BMC Neurol. 18 (1), 67.

Sormani, M.P., De Stefano, N., Giovannoni, G., Langdon, D., Piani-Meier, D., Haering, D. A., 2018. Learning ability correlates with brain atrophy and disability progression in RRMS. J. Neurol. Neurosurg. Psychiatry.

Damjanovic, D., Valsasina, P., Rocca, M.A., Stromillo, M.L., Gallo, A., Enzinger, C., 2017. Hippocampal and Deep Gray Matter Nuclei Atrophy Is Relevant for Explaining Cognitive Impairment in MS: a Multicenter Study. Am. J. Neuroradiol. 38 (1), 18–24.

Kincses, B., Spisák, T., Faragó, P., Király, A., Szabó, N., Veréb, D., 2020. Brain MRI Diffusion Encoding Direction Number Affects Tract-Based Spatial Statistics Results in Multiple Sclerosis. J. Neuroimaging 30 (4), 512–522.

Tóth, E., Faragó, P., Király, A., Szabó, N., Veréb, D., Kocsis, K., 2019. The Contribution of Various MRI Parameters to Clinical and Cognitive Disability in Multiple Sclerosis. Front Neurol 9, 1172.

Polman, C.H., Reingold, S.C., Edan, G., Filippi, M., Hartung, H.P., Kappos, L., 2005. Diagnostic criteria for multiple sclerosis: 2005 revisions to the "McDonald Criteria". Ann. Neurol. 58 (6), 840–846.

Behrens, T.E., Woolrich, M.W., Jenkinson, M., Johansen-Berg, H., Nunes, R.G., Clare, S., 2003. Characterization and propagation of uncertainty in diffusion-weighted MR imaging. Magn. Reson. Med. 50 (5), 1077–1088.

Smith, S.M., Jenkinson, M., Johansen-Berg, H., Rueckert, D., Nichols, T.E., Mackay, C.E., 2006. Tract-based spatial statistics: voxelwise analysis of multi-subject diffusion data. Neuroimage 31 (4), 1487–1505.

McIntosh, A.R., Lobaugh, N.J., 2004. Partial least squares analysis of neuroimaging data: applications and advances. Neuroimage 23, S250–S263. Suppl 1.

Aliotta, R., Cox, J.L., Donohue, K., Weinstock-Guttman, B., Yeh, E.A., Polak, P., 2014. Tract-based spatial statistics analysis of diffusion-tensor imaging data in pediatric- and adult-onset multiple sclerosis. Hum. Brain Mapp. 35 (1), 53–60.

Giorgio, A., Palace, J., Johansen-Berg, H., Smith, S.M., Ropele, S., Fuchs, S., 2010. Relationships of brain white matter microstructure with clinical and MR measures in relapsing-remitting multiple sclerosis. J. Magn. Reson. Imaging 31 (2), 309–316.

Velicu, I.L., Neagu, M., Dobromir, M., Luca, D., Lupu, N., Chiriac, H., 2012. Structural, Magnetic and Magnetoelastic Behaviour of FeCuNbSiB Thin Films. Sensor Lett. 10 (3–4), 902–905.

Song, S.K., Yoshino, J., Le, T.Q., Lin, S.J., Sun, S.W., Cross, A.H., 2005. Demyelination increases radial diffusivity in corpus callosum of mouse brain. Neuroimage 26 (1), 132–140.

Nocentini, U., Bozzali, M., Spano, B., Cercignani, M., Serra, L., Basile, B., 2012. Exploration of the relationships between regional grey matter atrophy and cognition in multiple sclerosis. Brain Imaging Behav.

Montalban, X., Sastre-Garriga, J., Tintore, M., Brieva, L., Aymerich, F.X., Rio, J., 2009. A single-center, randomized, double-blind, placebo-controlled study of interferon beta-1b on primary progressive and transitional multiple sclerosis. Mult. Scler. 15 (10), 1195–1205.

Perez-Miralles, F.C., Sastre-Garriga, J., Tintore, M., Nos, C., Perkal, H., Rio, J., 2009. Magnitude and clinical underpinnings of short-term tissue specific atrophy development in first attacks of multiple sclerosis. Mult. Scler. 15 (9). S221-S.

Senda, J., Watanabe, H., Tsuboi, T., Hara, K., Watanabe, H., Nakamura, R., 2012. MRI mean diffusivity detects widespread brain degeneration in multiple sclerosis. J. Neurol. Sci. 319 (1–2), 105–110.

Filippi, M., Cercignani, M., Inglese, M., Horsfield, M.A., Comi, G., 2001. Diffusion tensor magnetic resonance imaging in multiple sclerosis. Neurology 56 (3), 304–311.

Onu, M., Roceanu, A., Sboto-Frankenstein, U., Bendic, R., Tarta, E., Preoteasa, F., 2012. Diffusion abnormality maps in demyelinating disease: correlations with clinical scores. Eur. J. Radiol. 81 (3), e386–e391.

Ciccarelli, O., Werring, D.J., Wheeler-Kingshott, C.A.M., Barker, G.J., Parker, G.J.M., Thompson, A.J., 2001. Investigation of MS normal-appearing brain using diffusion tenser MRI with clinical correlations. Neurology 56 (7), 926–933.

Griffin, C.M., Chard, D.T., Ciccarelli, O., Kapoor, B., Barker, G.J., Thompson, A.I., 2001. Diffusion tensor imaging in early relapsing-remitting multiple sclerosis. Mult. Scler. 7 (5), 290–297.

Hasan, K.M., Gupta, R.K., Santos, R.M., Wolinsky, J.S., Narayana, P.A., 2005. Diffusion tensor fractional anisotropy of the normal-appearing seven segments of the corpus callosum in healthy adults and relapsing-remitting multiple sclerosis patients. J. Magn. Reson. Imaging 21 (6), 735–743.

Fricska-Nagy, Z., Fuvesi, J., Rozsa, C., Komoly, S., Jakab, G., Csepany, T., 2016. The effects of fatigue, depression and the level of disability on the health-related quality of life of glatiramer acetate-treated relapsing-remitting patients with multiple sclerosis in Hungary. Mult Scler Relat Dis 7, 26–32.

Blecher, T., Miron, S., Schneider, G.G., Achiron, A., Ben-Shachar, M, 2019. Association Between White Matter Microstructure and Verbal Fluency in Patients With Multiple Sclerosis. Front Psychol 10.

Abel, S., Vavasour, I., Lee, L.E., Johnson, P., Ackermans, N., Chan, J., 2019. Myelin Damage in Normal Appearing White Matter Contributes to Impaired Cognitive Processing Speed in Multiple Sclerosis. J. Neuroimaging.

Johnen, A., Schiffler, P., Landmeyer, N.C., Tenberge, J.G., Riepl, E., Wiendl, H., 2019. Resolving the cognitive clinico-radiological paradox - Microstructural degeneration of fronto-striatal-thalamic loops in early active multiple sclerosis. Cortex 121, 239–252.

Baumeister, T.R., Lin, S.J., Vavasour, I., Kolind, S., Kosaka, B., Li, D.K.B., 2019. Data fusion detects consistent relations between non-lesional white matter myelin, executive function, and clinical characteristics in multiple sclerosis. Neuroimage Clin 24, 101926.

Kincses, Z.T., Ropele, S., Jenkinson, M., Khalil, M., Petrovic, K., Loitfelder, M., 2011b. Lesion probability mapping to explain clinical deficits and cognitive performance in multiple sclerosis. Mult Scler J 17 (6), 681–689.

Toth, E., Farago, P., Kiraly, A., Szabo, N., Vereb, D., Kocsis, K., 2019. The Contribution of Various MRI Parameters to Clinical and Cognitive Disability in Multiple Sclerosis. Front Neurol 9.

McIntosh, A.R., Bookstein, F.L., Haxby, J.V., Grady, C.L., 1996. Spatial pattern analysis of functional brain images using partial least squares. Neuroimage 3, 143–157, 3 Pt 1.

Ge, S., Wang, R., Leng, Y., Wang, H., Lin, P., Iramina, K, 2017. A Double-Partial Least-Squares Model for the Detection of Steady-State Visual Evoked Potentials. IEEE J Biomed Health Inform 21 (4), 897–903.

Vytvarova, E., Marecek, R., Fousek, J., Strycek, O., Rektor, I., 2017. Large-scale cortico-subcortical functional networks in focal epilepsies: the role of the basal ganglia. Neuroimage Clin 14, 28–36.

Konukoglu, E., Coutu, J.P., Salat, D.H., Fischl, B., 2016. Adni. Multivariate statistical analysis of diffusion imaging parameters using partial least squares: application to white matter variations in Alzheimer's disease. Neuroimage 134, 573–586.

Park, B.Y., Seo, J., Yi, J., Park, H, 2015. Structural and Functional Brain Connectivity of People with Obesity and Prediction of Body Mass Index Using Connectivity. PLoS One 10 (11).